IOPscience iopscience.iop.org

Home Search Collections Journals About Contact us My IOPscience

Quantum stochastic Feynman rules and extended Wigner statistics

This article has been downloaded from IOPscience. Please scroll down to see the full text article.

1998 J. Phys. A: Math. Gen. 31 2021

(http://iopscience.iop.org/0305-4470/31/8/013)

View the table of contents for this issue, or go to the journal homepage for more

Download details:
IP Address: 171.66.16.104
The article was downloaded on 02/06/2010 at 07:23

Please note that terms and conditions apply.

J. Phys. A: Math. Gen. **31** (1998) 2021–2030. Printed in the UK PII: S0305-4470(98)82391-3

# Quantum stochastic Feynman rules and extended Wigner statistics

John Gough†

Department of Mathematical Physics, NUI Maynooth, Maynooth, Co. Kildare, Ireland

Received 6 March 1997, in final form 26 November 1997

**Abstract.** We introduce a Feynman diagram calculus for quantum stochastic fields and show that from the weak coupling limit of a Bose quantum field reservoir in a Gaussian state one obtains a quantum stochastic field process which has extended Wigner statistics. That is, we calculate explicitly the moments using the diagram rules and show that only moments corresponding to non-crossing diagrams are non-trivial. We further give the physical mechanism underlying this fact; namely the combination of momentum conservation (arising from the correct treatment of the full responsive interaction) and the mass-shell energy conservation for the virtual (stochastic) reservoir quanta. In our analysis we introduce a volume cut-off initially for the system particle to discretize its energy spectrum and then take the weak coupling limit. The individual noise fields associated with energy state transitions were Gaussian however, when the volume cut-off is then removed and we recover the noise correlations. Thus for this problem the removal of the cut-off and the weak coupling limit are in fact interchangeable.

## 1. Introduction

The weak coupling limit [4] is a well known device for obtaining a quantum stochastic description of a system coupled to a heat bath [5]. The limit description is either in terms of a master equation [6, 7] or equivalently in terms of quantum stochastic processes [3, 8, 9]. The weak coupling limit gives the *golden rule* of stochastic dynamics in which the Wigner–Weisskopf approximation becomes valid.

In the case where $S$ is an electron and $R$ is a phonon gas in a thermal state, for example, the interaction is responsive; that is, the electron couples differently to the different modes of the $R$. In particular, when the electron emits or absorbs a phonon it must recoil because of momentum conservation. In the unresponsive approximation this recoil is ignored and the information of momentum carried off by the phonon is lost. Whereas this is justifiable in the case of bound electron states, it can hardly be applied to conduction states. In the quantum electrodynamics (QED) case this corresponds, of course, to the dipole approximation. The treatments mentioned above assume an unresponsive interaction before passing to the weak coupling limit. In [3], however, a quantum stochastic evolution is obtained for an electron coupled to a thermal QED field without recourse to the dipole approximation. Here the system unperturbed Hamiltonian was discrete. The problem of treating a system with a continuous spectrum was studied in [1]. The limit noise had two novel features; it had to be considered as a function of the system particle's momentum and had non-Gaussian statistics. Specifically, only non-crossing moments of the noise were non-zero.

† E-mail address: jgough@thphys.may.ie

0305-4470/98/082021+10$19.50 © 1998 IOP Publishing Ltd 

The first quantum stochastic limit exhibiting this feature was the random matrix theory of Wigner [10] which introduced a non-commutative central limit theorem for which the limit law was not the standard Gaussian but the semi-circle law. We shall use the term *extended Wigner law* for the distribution of any process having only non-crossing moments different from zero. The limit noise of Accardi and Lu [1] is a modified version of those studied by Voiculescu [11] and Kümmerer and Speicher [12].

We give a physical explanation of why the weak coupling limit for continuous spectrum systems lead to such an extended Wigner law for the limit noise. We consider the full responsive interaction of a quantum field $R$ with the system; that is we do not make the dipole approximation. Instead we introduce a volume cut-off for the system (though not the reservoir) and use the results of [3] to describe the noise. Explicit diagram rules of Feynman character are given to calculate the noise moments; these we call the (finite volume) *stochastic Feynman diagrams*. We then remove the volume cut-off. It is then shown that the crossing diagrams vanish. Essentially the volume of momentum phase space for the $R$ quanta momenta vanishes. The moments corresponding to the non-crossing diagrams are calculated and are compared with those of Accardi and Lu [1].

The analysis of [3] and [2] both lead to limit stochastic descriptions for the case of fully responsive interactions; the former paper considering a system with discrete energy spectrum while the latter continuous. The noise statistics for the former was still Gaussian. This paper therefore answers how these two approaches are actually in accord.

## 2. System and reservoir

We consider a quantum mechanical system $S$ coupled to a bosonic quantum field reservoir $R$. The creation and annihilation operators for a reservoir quantum of wavevector $\boldsymbol{k}$ are denoted $b^\dagger(\boldsymbol{k})$ and $b(\boldsymbol{k})$, respectively, and we have the CCR $[b(\boldsymbol{k}), b^\dagger(\boldsymbol{k}')] = \delta(\boldsymbol{k}-\boldsymbol{k}')$. Here and in the following we shall suppress all internal degrees of the reservoir quanta such as spin or polarization. The total Hamiltonian is $H_\lambda = H_{\rm S} + H_{\rm R} + \lambda H_{\rm I}$, $H_{\rm S}$ and $H_{\rm R}$ being the unperturbed system and reservoir Hamiltonians, respectively. In particular, $H_{\rm R} = \int {\rm d}^3k\, \hbar\omega(\boldsymbol{k}) b^\dagger(\boldsymbol{k}) b(\boldsymbol{k})$.

The interaction $H_{\rm I}$ is taken to be linear in the reservoir quanta, that is $H_{\rm I} = {\rm i}\hbar\{A^\dagger - A\}$ where

$$A^\dagger = \int {\rm d}^3k\, \theta(\boldsymbol{k}) \otimes b^\dagger(\boldsymbol{k}). \tag{2.1}$$

Here $\theta(\boldsymbol{k})$ is a bounded operator on the system state space giving the response of the system to the creation of a reservoir quantum of momentum $\hbar\boldsymbol{k}$. The responseless approximation is to take $\theta(\boldsymbol{k}) \approx g(\boldsymbol{k})\Theta$ where $\Theta$ is a fixed operator on the system state space and $g(\boldsymbol{k})$ is a real-valued function. In this case, $A^\dagger = \Theta \otimes B^\dagger(g)$ where $B^\dagger(g) := \int {\rm d}^3k\, g(\boldsymbol{k}) b^\dagger(\boldsymbol{k})$.

Suppose that $H_{\rm S}$ has a discrete spectrum and assume the existence of a complete orthonormal basis $B$ of energy-eigenstates such that $H_{\rm S}|\phi\rangle = \hbar\epsilon(\phi)\ |\phi\rangle$ for each $\phi \in B$. The response may then be expanded in the form

$$\theta(\boldsymbol{k}) = \sum_{\phi,\phi'\in B} g_{\phi\phi'}(\boldsymbol{k}) |\phi\rangle\langle\phi'| \tag{2.2}$$

where we have the test function $g_{\phi\phi'}(\boldsymbol{k}) = \langle\phi|\theta(\boldsymbol{k})|\phi'\rangle$. The operator $A^\dagger$ may therefore be expanded as

$$A^\dagger = \sum_{\phi,\phi'\in B} |\phi\rangle\langle\phi'| \otimes B^\dagger(g_{\phi\phi'}). \tag{2.3}$$

Let $v_t^0(.)$ denote the unperturbed evolution superoperator then

$$v_t^0(A^\dagger) = \sum_{\phi,\phi' \in B} |\phi\rangle\langle\phi'| \otimes B^\dagger(S_t^{\omega_{\phi\phi'}} g_{\phi\phi'}) \tag{2.4}$$

where $(S_t^\omega g)(\boldsymbol{k}) := \mathrm{e}^{\mathrm{i}(\omega(\boldsymbol{k})-\omega)t} g(\boldsymbol{k})$ and we have introduced the Bohr frequency $\omega_{\phi\phi'} = \epsilon(\phi') - \epsilon(\phi)$ between energy states.

## 3. The weak coupling limit for a responsive interaction

The unitary operator

$$U_t^{(\lambda)} = T \exp\left\{\frac{\lambda}{\mathrm{i}\hbar}\int_0^t \mathrm{d}s\, v_s^0(H_\mathrm{I})\right\}$$

transforms to the interaction picture. In the weak coupling limit one studies the limit dynamics of the time-rescaled process $U_{t/\lambda^2}^{(\lambda)}$ as $\lambda \to 0$. In [3] this limit was studied for the set-up in the previous section and a unitary evolution was found with a Lindblad generator (for $X$ a system observable) $\mathcal{L}(X) = -XY - Y^\dagger X + \Theta(X)$ where the operator $Y$ gives the complex damping calculated by second-order perturbation theory. Explicitly we have, for $\phi \in B$ and the standard response term encountered in practice $\theta(\boldsymbol{k}) = f(\boldsymbol{k})\mathrm{e}^{-\mathrm{i}\boldsymbol{k}\cdot\boldsymbol{r}}$, that

$$\langle\phi, Y\phi\rangle = \frac{\hbar}{\mathrm{i}}\int \mathrm{d}^3k\, \langle\phi|\frac{N(\boldsymbol{k})+1}{\mathcal{D}^+(\phi,\boldsymbol{k}) - \mathrm{i}0^+} + \frac{N(\boldsymbol{k})}{\mathcal{D}^-(\phi,\boldsymbol{k}) - \mathrm{i}0^+}|\phi\rangle|f(\boldsymbol{k})|^2 \tag{3.1}$$

where $N(\boldsymbol{k})$ is the number density of particles with wavevector $\boldsymbol{k}$ and

$$\mathcal{D}^\pm(\phi,\boldsymbol{k}) = H_\mathrm{S} \mp \frac{\hbar\boldsymbol{p}\cdot\boldsymbol{k}}{m} + \frac{\hbar^2k^2}{2m} \pm \hbar\omega(\boldsymbol{k}) - E_\phi. \tag{3.2}$$

The first term in (3.1) gives the stimulated emission contribution while the second gives that of stimulated absorption.

As a physical model we consider an electron in a metal close to the lower edge of a conduction band [5]. Let $\phi = |\boldsymbol{l}\rangle$ be the eigenstate of momentum $\hbar\boldsymbol{l}$ such that $H_\mathrm{S}|\boldsymbol{l}\rangle = \hbar\epsilon(\boldsymbol{l})|\boldsymbol{l}\rangle$ where $\epsilon(\boldsymbol{l}) = (\hbar l^2/2m)$ is a good approximation for small values of $\boldsymbol{l}$. The interacting quantum field can be taken to be a phonon gas with acoustic dispersion law $\omega(\boldsymbol{k}) = c|\boldsymbol{k}|$ where $c$ is the speed of sound. The complex damping for state $|\boldsymbol{l}\rangle$ is calculated from (3.1) with the functions (3.2) replaced by

$$\mathcal{D}^\pm(\boldsymbol{l},\boldsymbol{k}) = \mp\frac{\hbar^2\boldsymbol{l}\cdot\boldsymbol{k}}{m} + \frac{\hbar^2k^2}{2m} \pm \hbar ck. \tag{3.3}$$

The actual damping, i.e. the real part of $\langle\boldsymbol{l}|Y|\boldsymbol{l}\rangle$, appears in the form of integrations over the respective spaces (mass shells) $\Sigma^\pm(\boldsymbol{l}) = \{\boldsymbol{k} \neq \boldsymbol{0} : \mathcal{D}^\pm(\boldsymbol{l},\boldsymbol{k}) = 0\}$.

In general, $\Sigma^\pm(\boldsymbol{l})$ is a two-dimensional hypersurface in $\boldsymbol{R}^3$ consisting of all vectors $\boldsymbol{k}$ such that $|\boldsymbol{k}| = \mp(l\cos\theta - (mc/\hbar))$ where $\theta$ is the angle between $\boldsymbol{l}$ and $\boldsymbol{k}$. Note that $\Sigma^+(\boldsymbol{l})$ is empty for $|\boldsymbol{l}| \leqslant (mc/\hbar)$ which means that the corresponding component of the damping is non-zero only for electron velocities in excess of the speed of sound.

The final result for the damping (also equivalent to the transition rate for state $\boldsymbol{l}$ from the golden rule) is that calculated by other authors, for example, Haken, cf [13, sections 29 and 30] and references within, where Frölich's Hamiltonian for electrons in interaction with phonons is considered. In the subsequent sections of this paper the moments of the limit noise are related to the damping coefficients and so we must have non-zero damping for non-trivial results. For an account of the renormalization see [13] or for a more rigorous treatment [14].

We remark that this theory is not applicable for QED as there is no damping: in general, we encounter the functions

$$\mathcal{D}^{\pm}(\boldsymbol{l},\boldsymbol{k}) = \overline{h}\epsilon(\boldsymbol{l}\mp\boldsymbol{k}) - \overline{h}\epsilon(\boldsymbol{l}) \pm \overline{h}\omega(\boldsymbol{k}). \tag{3.4}$$

However, for $\overline{h}\epsilon(\boldsymbol{l}) = \sqrt{m^2c^4 + c^2\overline{h}^2l^2}$ and $\omega(\boldsymbol{k}) = c|\boldsymbol{k}|$, the spaces $\Sigma^{\pm}(\boldsymbol{l})$ always consist of just the vector $\boldsymbol{k} = \boldsymbol{0}$, for all $\boldsymbol{l}$, which just signifies that the fundamental vertex of QED does not conserve four-momentum.

As is well known, there is a natural way of describing the creation and annihilation operators in a thermal state in terms of a pair of similar operators both in a vacuum state: $B(g) \equiv B_{\rm e}(Q_+g)\otimes 1 + 1\otimes B_{\rm a}^{\dagger}(Q_-g)$, where $((Q_{\pm}1)/2)^{1/2}$. The indices e and a stand for stimulated emission and absorption, respectively. In the remainder of this paper we shall understand $B^{\sharp}(g)$ to mean either the creation and annihilation fields in the vacuum state or either one of the stimulated emission or absorption states in their respective vacuum state for a thermal state.

## 4. The weak coupling limit

We now outline briefly the results concerning the weak coupling limit that we shall need. For further details concerning the exact construction of the noise spaces and the notion of convergence as a non-commutative process used see [3, 9].

*Theorem 1.* As a non-commutative central limit we have

$$\lim_{\lambda\to 0}\lambda\int_0^{t/\lambda^2} {\rm d}u\; B^{\sharp}(S_u^{\omega}g) = B_{\omega}^{\sharp}(g,t) \tag{4.1}$$

the limit is a quantum Wiener process [8] with commutation relations

$$[B_{\omega}(g,t),\, B_{\omega'}^{\dagger}(g',t')] = \delta_{\omega,\omega'}\, t\wedge t'(g|g')_{\omega} \tag{4.2}$$

where we have

$$(g|g')_{\omega} = \int {\rm d}^3k\, 2\pi\, \overline{g(k)}\,\delta(\omega(k)-\omega)\, g'(k). \tag{4.3}$$

*Corollary.* We have the following decomposition in terms of energy-state transitions on $S$

$$A_T^{\dagger} := \lim_{\lambda\to 0}\lambda\int_0^{T/\lambda^2} {\rm d}u\; v_u^0(A^{\dagger}) = \sum_{\phi,\phi'\in B} |\phi\rangle\langle\phi'|\otimes B_{\omega_{\phi\phi'}}^{\dagger}(g_{\phi\phi'},T). \tag{4.4}$$

The fields $A_T^{\sharp}$ are referred to as the *interaction noises*. The operators $A^{\sharp}$ live on the combined system–reservoir state space and therefore do not satisfy any CCR as such.

*Theorem 2.*

$$\lim_{\lambda\to 0} U_{t/\lambda^2}^{(\lambda)} = U_t \tag{4.5}$$

where $U_t$ is the unitary quantum stochastic process satisfying the differential equation

$${\rm d}U_t = \{{\rm d}A_t^{\dagger} - {\rm d}A_t - Y\otimes {\rm d}t\}U_t \tag{4.6}$$

with $U_0 = 1$.

The integrators in (4.6) are given by

$${\rm d}A^{\dagger}(t) = \sum_{\phi,\phi'\in B} |\phi\rangle\langle\phi'|\otimes {\rm d}B_{\omega_{\phi\phi'}}^{\dagger}(g_{\phi\phi'},t). \tag{4.7}$$

*Theorem 3.* For $X$ a bounded operator on the system state space, we have

$$\lim_{\lambda\to 0} U^{(\lambda)\dagger}_{t/\lambda^2}(X\otimes 1)U^{(\lambda)}_{t/\lambda^2} = U_t^\dagger (X\otimes 1)U_t. \tag{4.8}$$

## 5. Stochastic diagram rules

We wish to give diagram rules for computing $N$-point correlation functions of the type

$$\langle A^{\sharp_1}_{T_1}\dots A^{\sharp_N}_{T_N}\rangle. \tag{5.1}$$

By $\langle . \rangle$ we mean the expectation over the noise Fock vacuum defines as an operator on the system state space. We use the term *stochastic Feynman diagrams* to indicate that we have already taken the quantum stochastic limit of the field we wish to describe by diagram calculus. Clearly we must have $N = 2n$ and $n$ $A^\dagger$'s and $n$ $A$'s if (5.1) is to be non-zero. To see what can happen, we examine the two-point correlation

$$\begin{aligned}\langle A_{T_2}A^\dagger_{T_1}\rangle &= \sum_{\phi,\phi'\in B}\sum_{\psi,\psi'\in B}|\psi\rangle\langle\psi'|\phi'\rangle\langle\phi|\,\langle B_{\omega_{\psi'\psi}}(g_{\psi'\psi},T_2),B^\dagger_{\omega_{\phi'\phi}}(g_{\phi'\phi},T_1)\rangle\\ &= \sum_{\phi,\psi\in B}^{\epsilon(\phi)=\epsilon(\psi)}\sum_{\phi'\in B}|\psi\rangle\langle\phi|\,(T_1\wedge T_2)\int \mathrm{d}^3k\,\overline{g_{\phi'\psi}(\boldsymbol{k})}g_{\phi'\phi}(\boldsymbol{k})\,2\pi\delta(\omega(\boldsymbol{k})-\omega_{\phi'\phi}).\end{aligned} \tag{5.2}$$

We shall now give the rules for calculating the diagrams corresponding to given $2n$-point functions. We shall of course consider only non-trivial diagrams. With the operator $|\psi\rangle\langle\phi|\otimes B^\dagger_\omega(g,t)$ we associate the vertex (figure 1).

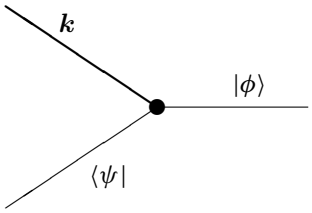


**Figure 1.** The vertex $A^\dagger$.

The system particle is denoted with a thin line while the $R$-quanta is denoted with a thick line. We shall adopt the convention throughout that all diagrams read from right to left and we note that every vertex is labelled by a time variable. The time variables appearing in a diagram are not necessarily in increasing order as we read from right to left.

For an arbitrary sub-diagram we draw generically a box (figure 2) with a broken boundary, while for a sub-diagram having no external lines of the $R$-quanta (i.e. there are no reservoir quanta which are emitted without being subsequently re-absorbed in the sub-diagram and *vice versa*) then we reserve the diagram (figure 3) of a box with a full boundary.

**Figure 2.** Arbitrary diagram.

**Figure 3.** Diagram with no external $R$-quanta.

*Rule 1.* With (figure 1) multiply by $g_{\phi\psi}(\boldsymbol{k})$: with its mirror image multiply by $\overline{g_{\phi\psi}(\boldsymbol{k})}$.

*Rule 2.* For the situation where $\phi$ and $\psi$ are input and output states for a diagram with no other external system or reservoir quanta lines, we must have $\epsilon(\phi) = \epsilon(\psi)$.

*Rule 3.* For a reservoir quantum which is emitted and re-absorbed along the same line (figure 4), multiply by $(T \wedge S)\,\delta(\omega_{\phi\phi'} - \omega_{\psi\psi'})\,2\pi\delta(\omega(\boldsymbol{k}) - \omega_{\phi\phi'})$.


**Figure 4.** Contraction diagram.

*Rule 4.* Sum over all intermediate states (running through $B$) and integrate over all reservoir quanta momenta. Sum over the pair of external system states subject to rule 2.

For example, we may display the following $2n$-point functions as diagrams and use the above rules to calculate them. $\langle A_{T_2} A^\dagger_{T_1}\rangle$ is represented by (figure 5) while $\langle A_{T_4} A^\dagger_{T_3} A_{T_2} A^\dagger_{T_1}\rangle$ is by (figure 6) and $\langle A_{T_4} A_{T_3} A^\dagger_{T_2} A^\dagger_{T_1}\rangle$ by (figure 7).

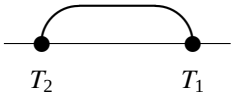


**Figure 5.** $\langle A_{T_2} A^\dagger_{T_1}\rangle$.

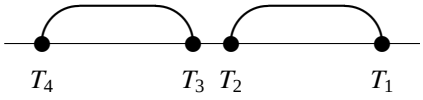


**Figure 6.** $\langle A_{T_4} A^\dagger_{T_3} A_{T_2} A^\dagger_{T_1}\rangle$.

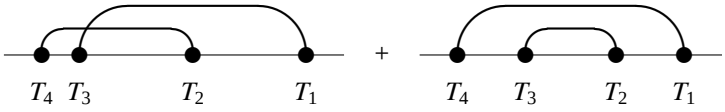


**Figure 7.** $\langle A_{T_4} A_{T_3} A^\dagger_{T_2} A^\dagger_{T_1}\rangle$.

## 6. The free particle limit

We consider a free particle in a box $V = L \times L \times L$ with Hamiltonian $H_{\rm S} = (1/2m)p^2$. Let $V^* = ((2\pi/L)\boldsymbol{Z})^3$, then assuming periodic boundary conditions we have a basis $B = \{|\boldsymbol{l}\rangle : \boldsymbol{l} \in V^*\}$ where $\langle \boldsymbol{r}|\boldsymbol{l}\rangle := (1/V^{-1/2})\,{\rm e}^{{\rm i}\boldsymbol{l}\cdot\boldsymbol{r}}$. Here we have $H_{\rm S}|\boldsymbol{l}\rangle = \overline{h}\epsilon(\boldsymbol{l})|\boldsymbol{l}\rangle$ where $\epsilon(\boldsymbol{l}) = (\overline{h}/2m)l^2$. Now, as is standard in most models, we take the response to be

$$\theta(\boldsymbol{k}) := {\rm e}^{-{\rm i}\boldsymbol{k}\cdot\boldsymbol{r}} f(\boldsymbol{k}). \tag{6.1}$$

The test functions for the interaction are then given by

$$g_{l'l}(\boldsymbol{k}) = \langle \boldsymbol{l}'|\theta(\boldsymbol{k})|\boldsymbol{l}\rangle = \int_V {\rm d}^3 r\, \frac{{\rm e}^{{\rm i}(\boldsymbol{l}-\boldsymbol{k}-\boldsymbol{l}')\cdot\boldsymbol{r}}}{V} f(\boldsymbol{k}) =: \frac{(2\pi)^3}{V}\delta_V(\boldsymbol{l}-\boldsymbol{k}-\boldsymbol{l}')f(\boldsymbol{k}). \tag{6.2}$$

Here $\delta_V$ is a regularization of the delta function. In the continuum limit ($V \to \infty$) we clearly obtain the constraint $\boldsymbol{l}' = \boldsymbol{l} - \boldsymbol{k}$ which is of course nothing more than momentum conservation: the diagram rules for the infinite volume limit are analogous to the earlier ones. In the continuum of states limit, the sum over intermediate momentum states is replaced by an integration in rule 4. Similarly, the fundamental vertex has strict momentum conservation built in and we understand rule 1 to mean that we multiply by $f(\boldsymbol{k})$. Thus we have figure 1 with $|\phi\rangle = |\boldsymbol{l}\rangle$ and $\langle\psi| = \langle\boldsymbol{l} - \boldsymbol{k}|$. We shall now calculate the 2-point function in the continuum limit: note first of all that we have, for suitable functions $h = h(\boldsymbol{l})$,

$$\lim_{V\to\infty} \frac{(2\pi)^3}{V} \sum_{\boldsymbol{l}\in V^*} h(\boldsymbol{l}) = \int_{\boldsymbol{R}^3} \mathrm{d}^3 l\, h(\boldsymbol{l}). \tag{6.3}$$

From (5.2) we have

$$\langle A_{T_2} A^\dagger_{T_1}\rangle = (T_1 \wedge T_2) \sum_{\boldsymbol{l},\boldsymbol{l}'\in V^*}^{\epsilon(\boldsymbol{l})=\epsilon(\boldsymbol{l}')} \sum_{\boldsymbol{l}_1\in V^*} \int \mathrm{d}^3 k\, |\boldsymbol{l}\rangle\langle\boldsymbol{l}'| \frac{(2\pi)^3}{V}$$
$$\times \delta_V(\boldsymbol{l} - \boldsymbol{k} - \boldsymbol{l}_1) \frac{(2\pi)^3}{V} \delta_V(\boldsymbol{l}' - \boldsymbol{k} - \boldsymbol{l}_1) |f(\boldsymbol{k})|^2\, 2\pi\delta(\omega(\boldsymbol{k}) - \epsilon(\boldsymbol{l}_1) + \epsilon(\boldsymbol{l})) \tag{6.4a}$$

$$\to (T_1 \wedge T_2) \int \mathrm{d}r \int \mathrm{d}\Omega \int \mathrm{d}\Omega' \int \mathrm{d}r_1 \int \mathrm{d}\Omega_1 \int \mathrm{d}^3 k\, |\boldsymbol{l}\rangle\langle\boldsymbol{l}'|$$
$$\times |f(\boldsymbol{k})|^2\, 2\pi\delta(\omega(\boldsymbol{k}) - \epsilon(\boldsymbol{l}_1) + \epsilon(\boldsymbol{l})) \tag{6.4b}$$

where in (6.4*b*) $\boldsymbol{l} = (r, \Omega)$, $\boldsymbol{l}' = (r, \Omega')$ and $\boldsymbol{l}_1 = (r_1, \Omega_1)$ in polar coordinates. Performing the $\boldsymbol{l}_1 = (r_1, \Omega_1)$ integration and integrating out the $\delta(\Omega - \Omega')$ which arises, we obtain as the infinite volume limit

$$(T_1 \wedge T_2) \int \mathrm{d}l \int \mathrm{d}k\, |\boldsymbol{l}\rangle\langle\boldsymbol{l}|\, |f(\boldsymbol{k})|^2\, 2\pi\delta(\omega(\boldsymbol{k}) - \epsilon(\boldsymbol{l} - \boldsymbol{k}) + \epsilon(\boldsymbol{l})). \tag{6.5}$$

We now show that all crossing diagrams in the continuum limit vanish. First we consider the simplest situation; corresponding to $\langle A_{T_4} A_{T_3} A^\dagger_{T_2} A^\dagger_{T_1}\rangle$. We have to consider two diagrams; the non-crossing diagram after the continuum limit (if we include all momenta conservation constraints) is as given in (figure 8). Note that the Bohr frequencies match between each pair of emission and absorption vertices; this is required by rule 3.

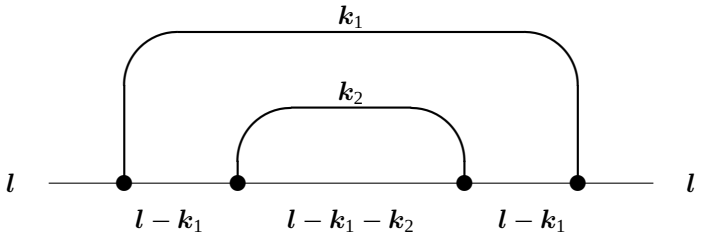


**Figure 8.** Non-crossing component of $\langle A_{T_4} A_{T_3} A^\dagger_{T_2} A^\dagger_{T_1}\rangle$.

Rule 4 need only be modified to integrate the system particle's momenta $\boldsymbol{l}$ over $\boldsymbol{R}^3$ due to the continuum limit. The value associated to this diagram is non-zero and readily computed.

If on the other hand we examine the crossing diagram (figure 9) we see that the condition for the Bohr frequencies to match between vertices at $T_1$ and $T_3$ is

$$\epsilon(\boldsymbol{l}) - \epsilon(\boldsymbol{l} - \boldsymbol{k}_1) = \epsilon(\boldsymbol{l} - \boldsymbol{k}_2) - \epsilon(\boldsymbol{l} - \boldsymbol{k}_1 - \boldsymbol{k}_2) \tag{6.6}$$

or equivalently

$$\boldsymbol{k}_1 \cdot \boldsymbol{k}_2 = 0. \tag{6.7}$$

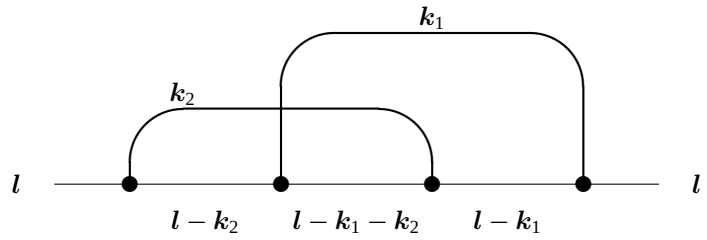


**Figure 9.** Crossing component of $\langle A_{T_4} A_{T_3} A^\dagger_{T_2} A^\dagger_{T_1}\rangle$.

However, since (6.7) only holds for a set of zero measure in $\boldsymbol{R}^3 \times \boldsymbol{R}^3$, we have that the diagram is in fact vanishing.

The condition for a diagram to be non-zero in the continuum limit is given as an extra rule.

*Rule 5.* Whenever we have an emission and re-absorption of a reservoir quantum, the intermediate sub-diagram cannot have any external lines of other reservoir quanta (figure 10): this is the only way to satisfy all the momentum conservation requirements at each vertex and, in addition, the vertex to vertex energy conservation of all pairs of emissions and absorptions.

Put more simply: the only diagram corresponding to a $2n$-point function which survives the continuum limit is the non-crossing diagram. (If a non-crossing diagram exists for a given $2n$-point function then it is necessarily unique.)

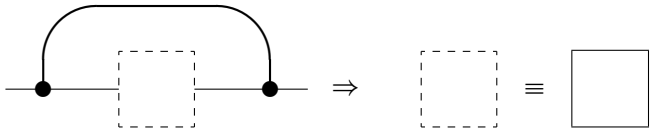


non-trivial

**Figure 10.**

If $\langle A^{\sharp_{2n}}_{T_{2n}} \dots A^{\sharp_1}_{T_1}\rangle$ is non-zero then consider the ordered sequence of creator index positions $M = (m_n, \dots, m_1)$ such that $\sharp_{m_j} = \dagger$, $j = 1, \dots, n$, and $m_h < m_{h+1}$, for $h = 1, \dots, n-1$. The possible positions of the annihilators are given by $M^c = \{1, \dots, 2n\}/M$. We must have $\sharp\{\overline{m} \in M^c : \overline{m} \leqslant r\} \leqslant \max\{h : m_h \leqslant r\}$, for all $r = 1, \dots, 2n$, otherwise the $2n$-point function vanishes.

There is only one sequence $(\overline{m}_n, \dots, \overline{m}_1)$ equivalent to $M^c$ as a set with $\overline{m}_h > m_h$, $h = 1, \dots, n$, which satisfies the conditions that whenever $\overline{m}_h > m_j > m_h$ then $\overline{m}_h > \overline{m}_j > m_h$ and that whenever $\overline{m}_h > \overline{m}_j > m_h$ then $\overline{m}_h > m_j > m_h$.

The pair partition $\{(m_h, \overline{m}_h) : h = 1, \dots, n\}$ of $\{1, \dots, 2n\}$ is called the Wigner or admissible pair partition for the set $\{\sharp_{2n}, \dots, \sharp_1\}$. These pairings give precisely the non-crossing diagram associated with $\langle A^{\sharp_{2n}}_{T_{2n}} \dots A^{\sharp_1}_{T_1}\rangle$. It is straightforward to show from the

diagram rules for the continuum case that

$$\langle A^{\sharp_{2n}}_{T_{2n}} \dots A^{\sharp_1}_{T_1} \rangle = \prod_{j=1}^{n} \min(T_{\overline{m}_j}, T_{m_j}) \int \mathrm{d}^3 l \, |\boldsymbol{l}\rangle\langle\boldsymbol{l}| \int \mathrm{d}k_{m_1} \dots \int \mathrm{d}k_{m_n} \int \mathrm{d}\tau_1 \dots$$
$$\times \int \mathrm{d}\tau_n \prod_{h=1}^{n} |f(\boldsymbol{k}_{m_h})|^2 \mathrm{e}^{\mathrm{i}\Delta(\boldsymbol{l}_{m_h}, \boldsymbol{k}_{m_h})\tau_h}. \tag{6.8}$$

Note that the diagrams correspond to operators which are diagonal in the momentum representation, as expected from the conservation of momentum. In (6.10) we have introduced the energy violation function $\Delta(\boldsymbol{l}, \boldsymbol{k})$ for the vertex defined by $\overline{h}\Delta(\boldsymbol{l}, \boldsymbol{k}) = \mathcal{D}^+(\boldsymbol{l}, \boldsymbol{k})$

$$\Delta(\boldsymbol{l}, \boldsymbol{k}) := \omega(\boldsymbol{k}) + \epsilon(\boldsymbol{l} - \boldsymbol{k}) - \epsilon(\boldsymbol{l}) \equiv \omega(\boldsymbol{k}) + \frac{\overline{h}}{2m}k^2 - \frac{\overline{h}}{m}\boldsymbol{l} \cdot \boldsymbol{k}. \tag{6.9}$$

Also in (6.8) we have introduced the momentum $\boldsymbol{l}_{m_h}$ of the system particle immediately after the emission vertex at $T_{m_h}$. With $\boldsymbol{k}_{m_j}$ denoting the momentum of the reservoir quantum emitted at $T_{m_j}$ and, of course, absorbed at $T_{\overline{m}_j}$ (so $\boldsymbol{k}_{\overline{m}_j} = \boldsymbol{k}_{m_j}$), and using the convention that $(-1)^\sharp = 1$ if $\sharp = \dagger$ and $-1$, otherwise we have that

$$\boldsymbol{l}_{m_h} \equiv \boldsymbol{l} - \sum_{j=1}^{m_h - 1} (-1)^{\sharp_j} \boldsymbol{k}_j \tag{6.10}$$

for the non-crossing diagrams. It is easy to see that (6.12) can be rewritten as

$$\boldsymbol{l}_{m_h} = \boldsymbol{l} - \sum_{r}^{m_h < m_r < \overline{m}_h} \boldsymbol{k}_{m_r}. \tag{6.11}$$

Therefore, we have that

$$\Delta(\boldsymbol{l}_{m_h}, \boldsymbol{k}_{m_h}) = \omega(\boldsymbol{k}_{m_h}) + \frac{\overline{h}}{2m}k^2_{m_h} - \frac{\overline{h}}{m}\boldsymbol{l} \cdot \boldsymbol{k}_{m_h} + \frac{\overline{h}}{m} \sum_{r}^{m_h < m_r < \overline{m}_h} \boldsymbol{k}_{m_r} \cdot \boldsymbol{k}_{m_h}. \tag{6.12}$$

Substituting (6.12) into (6.8) gives

$$\langle A^{\sharp_{2n}}_{T_{2n}} \dots A^{\sharp_1}_{T_1} \rangle = \prod_{j=1}^{n} \min(T_{\overline{m}_j}, T_{m_j}) \int \mathrm{d}^3 k_{m_1} \dots \int \mathrm{d}^3 k_{m_n} \int \mathrm{d}\tau_1 \dots \int \mathrm{d}\tau_n$$
$$\times \left\{ \prod_{h=1}^{n} |f(\boldsymbol{k}_{m_h})|^2 \mathrm{e}^{\mathrm{i}(\omega(\boldsymbol{k}_{m_h}) + (\overline{h}/2m)k^2_{m_h})\tau_h} \right\} \exp\left\{ \mathrm{i}\frac{1}{m}\boldsymbol{p} \cdot \sum_{j=1}^{n} \sum_{r=1}^{j-1} \boldsymbol{k}_{m_r}\tau_j \right\}$$
$$\times \exp\left\{ \mathrm{i}\frac{\overline{h}}{m} \sum_{r}^{m_h < m_r < \overline{m}_h} \boldsymbol{k}_{m_r} \cdot \boldsymbol{k}_{m_h} \right\}. \tag{6.13}$$

This agrees with the $2n$-point functions calculated by Accardi and Lu [1].

The survival of only non-crossing moments is therefore a universal phenomenon for interacting noises approximating the action of quantum field reservoirs with responsive interactions.

**Acknowledgments**

The author is very happy to thank Professors L Accardi and Y G Lu for many stimulating discussions during the writing of this paper and he also thanks Professor R Alicki for several useful and critical remarks about the physical interpretation.

## References


[1] Accardi L and Lu Y G 1996 The Wigner semi-circle law in quantum electro dynamics *Commun. Math. Phys.* **180** 3 605–32

[2] Gough J 1997 The interacting-free quantum stochastic limit of quantum field theory *J. Math. Phys.* **38** 867–81

[3] Accardi L, Gough J and Lu Y G 1995 On the stochastic limit for quantum field theory *Rev. Math. Phys.* **36** 155–87

[4] van Hove L 1955 Quantum mechanical perturbations giving rise to a statistical transport equation *Physica* **21** 617–40

[5] Alicki R 1978 The theory of open systems in application to unstable particles *Rev. Math. Phys.* **14** 27–42

[6] Davies E B 1974 Markovian master equations *Commun. Math. Phys.* **39** 91–110

[7] Gorini V, Frigerio A, Verri M, Kossakowski A and Sudarshan E C G 1978 Properties of Markovian master equations *Rev. Math. Phys.* **13** 149–73

[8] Hudson R L and Parthasarathy K R 1984 Quantum Ito's formula and stochastic evolutions *Commun. Math. Phys.* **93** 301–23

[9] Accardi L, Frigerio A and Lu Y G 1990 The weak coupling limit as a quantum functional central limit theorem *Commun. Math. Phys.* **131** 537–70

[10] Wigner E 1967 Random matrices *SIAM Rev.* **9** 1–23

[11] Voiculescu D 1991 *Free Non-commutative Random Variables, Random Matrices and the $II_1$ Factors of Free Groups (QP VI)* (New York: Springer) pp 473–88

[12] Kümmerer B and Speicher R 1992 Stochastic integration on the Cuntz algebra $\mathcal{O}_\infty$ *J. Funct. Anal.* **103** 372–408

[13] Haken H 1976 *Quantum Field Theory Of Solids* (Amsterdam: North-Holland)

[14] Davies E B 1979 Particle–boson interactions and the weak coupling limit *J. Math. Phys.* **20** 345–61